Journal of Materials Chemistry

Cite this: *J. Mater. Chem.*, 2012, **22**, 1511

www.rsc.org/materials

PAPER

Cu–Ge core–shell nanowire arrays as three-dimensional electrodes for high-rate capability lithium-ion batteries

Jiazheng Wang, Ning Du,* Hui Zhang, Jingxue Yu and Deren Yang

Received 7th September 2011, Accepted 28th October 2011
DOI: 10.1039/c1jm14430h

We demonstrate the synthesis of three-dimensional Cu–Ge core–shell nanowire array electrodes by directly depositing Ge on the surface of pre-synthesized Cu nanowire arrays *via* an rf-sputtering method. When used as anodes of lithium-ion batteries, the Cu–Ge nanowire arrays display a high capacity of 1419 mAh g^{-1} at 0.5 C after 40 cycles and 734 mAh g^{-1} at 60 C after 80 cycles, which is better than planar electrodes. The improved performance can be attributed to the good electrical contact, fast electron transport and good strain accommodation of the nanowire array electrodes. The effect of the thickness of Ge layer on the electrochemical performance of the three-dimensional electrodes has also been investigated.

Introduction

Currently, lithium-ion batteries are widely used in portable electronics and high power applications such as mobile phones, laptops, electric vehicles and so forth.[1–3] At present, graphite is used as the commercial anode material for lithium-ion batteries, however, it has a relatively low theoretical capacity (372 mAh g^{-1}) which greatly limits its further application.[4] Therefore, large research efforts are presently devoted to search for useful alternative materials with large capacity, low operating potentials, high-rate tolerance, and long cycle life.[5–10]

As the elements of the same family with carbon (group IV), silicon (Si) and germanium (Ge) are believed to be ideal candidates for anode materials of Li-ion batteries with theoretical capacities of 4200 and 1600 mAh g^{-1}, respectively.[11,12] Despite the high theoretical capacity, Si is confronted with the following problems, which may restrict its commercial application: (1) the 400% volume change during the alloying/dealloying process of lithiation leads to decrepitating and a loss of electrical contact;[13–15] (2) the slow kinetics of lithium transport in silicon limits the application of these anodes to medium and high-temperature cells using molten electrolytes;[14,16–18] (3) Si tends to form a native oxide on its outermost layers and the oxides resulting in the formation of a lithium inactive Li_2O phase during the first charge (lithium insertion), leading to a decrease in initial Coulombic efficiency. Compared to Si, Ge shows a minimal amount of native oxide in its outermost layer, exhibits a relatively low specific volume change and large diffusion coefficient during the Li insertion/extraction process.[19]

Nevertheless, an electrode based on the pure Ge still suffers from poor performance owing to large volume change and poor conductivity during the charge and discharge process, which ultimately leads to a dramatic capacity loss. Several strategies have been proposed to improve the cyclability of element-based materials such as dispersing Ge into an inactive matrix, decreasing the particle size, and using the elemental thin films or alloys.[20–23] These approaches can only improve the electrochemical performance of Ge anodes to a limited extent. More recently, it was reported that order-aligned nanostructured materials have significant advantages in their kinetics and electronic conduction during the alloying–dealloying process, compared to their bulky counterparts.[24–27] For example, L. Bazina, *et al.* reported a nano-architectured Sn anode for Li-ion battery, which delivered long cycle life and good power performance compared to planar tin films.[26] Scrosati and co-workers have prepared the 3D Ni–Sn nanostructured electrode by electrodeposition onto Cu nanorods, which exhibits stable cycling capacity (~500 mAh g^{-1}).[27] It is believed that the improved performance and high rate capability are due to the good electrical contact, fast electron transport and good strain accommodation of the order-aligned nanostructure.

Herein, we use the similar strategy to improve the electrochemical performance of Ge electrodes. Cu–Ge core–shell nanowire electrodes were synthesized by directly depositing a Ge layer on pre-synthesized Cu nanowire arrays *via* an rf-sputtering technique. When used as anode materials of Li-ion batteries, Cu–Ge core–shell nanowire electrodes show excellent electrochemical performance in terms of cycle stability and rate capability.

State Key Laboratory of Silicon Materials and Department of Materials Science and Engineering, Zhejiang University, Hangzhou, 310027, People's Republic of China. E-mail: dna1122@zju.edu.cn; Fax: +86 571 87952322; Tel: +86 571 87953190

Experimental section

Synthesis of Cu nanowire arrays on Cu substrate

Cu nanowire arrays on copper substrates were fabricated by cathodic electrodeposition with anodized aluminum oxide (AAO) templates by a LK2006A electrochemical work station. The AAO membranes were prepared by a two-step anodization process as described elsewhere.[10] The pore diameter of the as-prepared templates is estimated to be about 40–50 nm with a density of 10^{10} to 10^{11} pores cm^{-2}. The cathode Cu substrates were first mechanically polished with 1.0 μm alpha alumina and 0.25 μm gamma alumina polishing slurry. Then the cathodes were further ultrasonically cleaned in ethanol and a diluted HCl solution (10 vol%) and rinsed with deionized water. The polished cathode Cu foil, AAO, separator (filter paper soaked with electrolyte, Whatman) and the anode Cu disc were packed in sequence and assembled using two stainless-steel clamps. The outer parts of the copper anode and cathode were protected from dissolution or deposition by isolating adhesive films which is similar to the method previously reported.[24]

The electrolyte systems consisted of $CuSO_4 \cdot 5H_2O$ 100 g L^{-1}, $(NH_4)_2SO_4$ 10 g L^{-1}, diethylenetriamine (DETA) 40 g L^{-1}. All the reagents were used without further purification. The Cu nanowires were electrochemically deposited under cyclic voltammetry conditions by sweeping the potential from −0.8 V to −1.0 V at room temperature with a rate of 3 mV s^{-1}. After 80 cycles, the as-prepared samples were taken out from the electrolyte, immersed in 2 M NaOH solution for 1 h to remove the AAO templates, and then rinsed several times with deionized water and stored in a glove box filled with an argon atmosphere.

Synthesis of Cu–Ge three-dimensional electrodes on Cu substrates

Pure Ge layers were deposited on the surface of Cu nanowire arrays by the rf-sputtering of a 99.99% pure germanium target at a working pressure of 3 Pa. The sputtering power was 70 W and the substrates were kept at 200 °C. Four types of thickness-controlled Ge thin films were prepared for comparison by sputtering time of 16 min, 32 min, 48 min and 64 min, respectively.

Characterization and electrochemical measurement

The morphology and structure of the obtained samples were examined by scanning electron microscopy (SEM HITACH S4800) with an energy-dispersive X-ray spectrometer (EDX) and transmission electron microscopy (TEM, PHILIPS CM200). Electrochemical measurements were performed by coin type cells (CR2025) which were assembled in a glove box (Mbraun, labstar, Germany) under an argon atmosphere by directly using the as-synthesized Cu–Ge three-dimensional electrodes as the anodes. The counter electrode was lithium metal foil (15 mm in diameter), and the electrolyte solution was a 1 M solution of $LiPF_6$ in ethylene carbonate (EC) and Dimethyl carbonate (DMC) (1 : 1 by volume). Finally, the cells were then aged for 12 h before measurements.

A galvanostatic cycling test of the assembled cells was carried out on a Land CT2001A system in the potential range of 0.01–1.2 V at a discharge/charge current density of 800 mA g^{-1}. Cyclic voltammetry (CV) was recorded on an Arbin BT 2000 system at a scan rate of 0.1 mV s^{-1}.

Results and discussion

Fig. 1a shows the procedure for the stepwise fabrication of Cu–Ge core–shell nanowires on a Cu substrate. At first, the Cu nanowire arrays on a Cu substrate were fabricated by cathodic electrodeposition *via* an AAO template-assisted method. Then, a Ge layer was coated onto the surface of Cu nanowires by an rf-sputtering technique. Fig. 1b is a scanning electron microscopy (SEM) image of the as-prepared Cu nanowires. It can be seen that the nanowires with a smooth surface are well aligned and perpendicular to the Cu substrate. The diameter of the Cu nanowires is estimated to be about 40–50 nm with a length of 1–2 μm, which is much smaller than that of the previously reported Cu pillar nanoarrays (200–300 nm in diameter) on current collectors.[24] It is believed that the small-diameter nanowires on current collectors could support more active materials, suggests a more efficient electron transport path, and a faster electrolyte diffusion. Fig. 2a–c show the top and cross-sectional views of the SEM images of the as-prepared core–shell nanowire arrays with the sputtering time of 48 min. As observed, the surface of the Cu nanowires turned rough and the diameter of the as-prepared nanowires increased, indicating the formation of a uniformly distributed Ge layer. It is revealed from the EDS spectrum in Fig. 2d that Cu and Ge are the dominant elements, further confirming the synthesis of Cu–Ge core–shell nanowire arrays.

Transmission Electron Microscope (TEM) was employed to further verify the core–shell structure (Fig. 3). The nanowires were scraped out of the substrate, sonicated in ethanol, and deposited on Au grids for TEM characterization. It can be seen from Fig. 3a–c that a uniform Ge layer with the thickness of about 50 nm has been deposited onto Cu nanowires. The picture on the top-right of Fig. 3b is a high resolution TEM (HRTEM) image of the Cu–Ge nanowire, which shows that the core is very

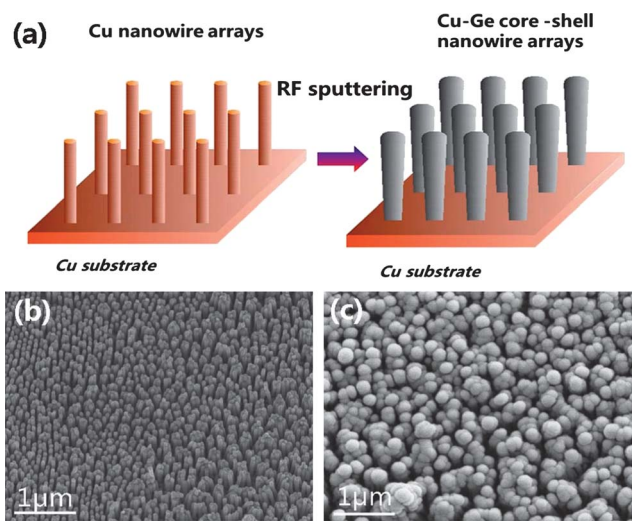

Fig. 1 (a) A schematic illustration for synthesis of the Cu–Ge three-dimensional electrode; (b) a SEM image of the Cu nanowire arrays on a current collector; (c) a SEM image of the Cu–Ge core–shell nanowire arrays.

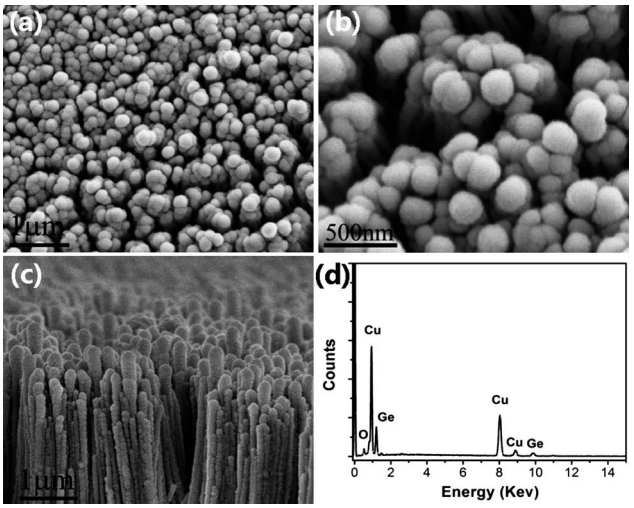

Fig. 2 (a), (b) Top-view SEM images of the Cu–Ge core–shell three-dimensional electrode fabricated by sputtering for 48 min; (c) Cross-section SEM images of the Cu–Ge core–shell three-dimensional electrode; (d) EDX spectrum of the Cu–Ge core–shell three-dimensional electrode.

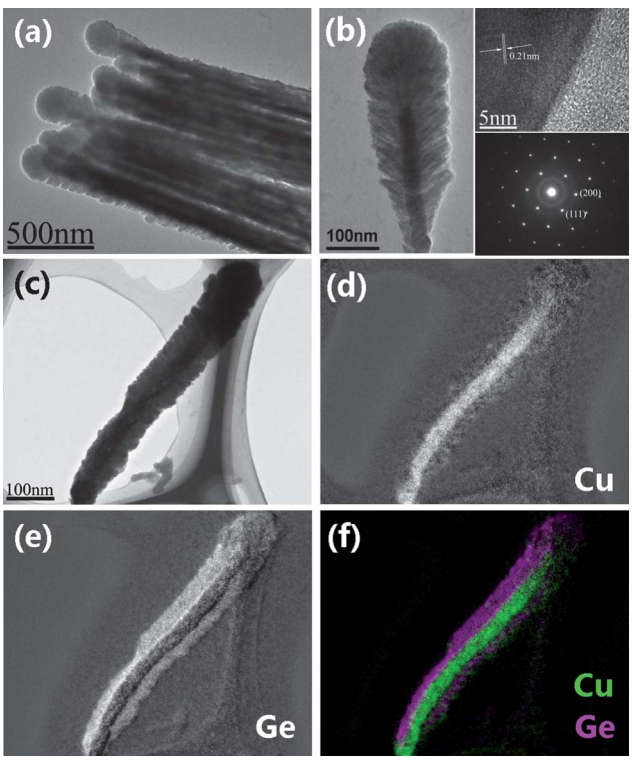

Fig. 3 (a) A TEM image of the Cu–Ge core–shell nanowire arrays; (b) a TEM image, HRTEM image and SAED pattern of an individual Cu–Ge core–shell nanowire; (c–f) a TEM and corresponding EELS elemental mapping (Cu, Ge, Cu/Ge) of an individual Cu–Ge core–shell nanowire.

crystalline and the shell is amorphous. The measured interplanar distance of the core is 0.21 nm, which corresponds to the Cu (111) planes. The dispersed selected-area electron diffraction (SAED) pattern (on the bottom-right of Fig. 3b) shows that the sputtered Ge shell is completely amorphous, which is in accordance with the HRTEM results. Fig. 3c and f display the TEM image of an individual Cu–Ge nanowire and the corresponding electron energy loss spectroscope (EELS) elemental mapping. It can be seen that Cu and Ge are evenly distributed in core and shell of the nanowire, respectively, further indicating the formation of uniform Cu–Ge core–shell nanowires.

Motivated by the unique structure of the core–shell nanowire arrays electrodes, we performed their electrochemical measurements. Fig. 4a represents the 1st, 2nd and 40th galvanostatic discharge/charge voltage profiles of the three-dimensional Cu–Ge electrodes. It can be seen that the Cu–Ge core–shell nanowire arrays electrodes deliver an initial discharge capacity of 1987 mAh g^{-1} and a reversible capacity of 1592 mAh g^{-1}, respectively, from which the Coulombic efficiency (the ratio between charge and discharge capacities) is calculated to be 80.1%. The large surface-to-volume ratio and the formation of the SEI film may be responsible for the high capacity in the first cycle, as evidenced by a voltage plateau at 0.6–0.85 V in Fig. 4a. The cell shows a reaction region with a plateau around 0.25 V, and the reaction ranges remain unchanged as the cycle number increased, which is consistent with the result of cyclic voltammetry (CV) measurements curves. CV measurements were carried out to understand electrochemical reactions during charging and discharging process. An insert in Fig. 4a shows the first three CV curves of the Cu–Ge nanowire array electrode at a scan rate of 0.1 mV s^{-1} and a temperature of 20 °C. During the discharge process, the peaks at 100–400 mV are associated with the formation of the Li–Ge alloy. The three cathodic peaks at 0.34 V, 0.18 V and 0.08 V derived from different lithium intercalation processes were observed in the second and third cycles. Upon charging, the peaks located at 0.41 V can be ascribed to the phase transition of Li_xGe to Ge. Fig. 4b shows the

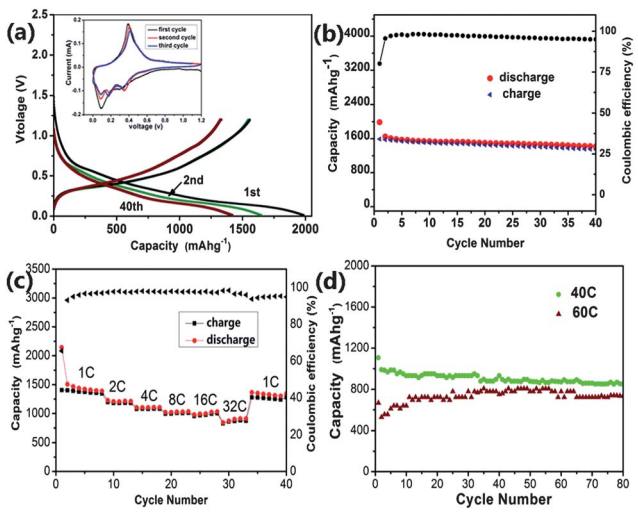

Fig. 4 (a) The galvanostatic discharge and charge voltage profiles of the Cu–Ge three-dimensional electrodes. An insert shows the first three CV curves at a scan rate of 0.1 mV s^{-1} and a temperature of 20 °C; (b) discharge and charge capacities *versus* cycle number for the Cu–Ge three-dimensional electrode at the current rate of 800 mA g^{-1}; (c) cycling performance at various C rates of the Cu–Ge three-dimensional electrode; (d) discharge and charge capacities *versus* cycle number for the Cu–Ge three-dimensional electrode at the rate of 40 C and 60 C, respectively.

charge/discharge capacity and Coulombic efficiency *versus* cycle numbers between 0.01 and 1.2 V at a constant current density of 800 mA g^{-1}. We notice that the Coulombic efficiency reached 95% at the second cycle while the others keep steadily above 97% thereafter. This can be ascribed to the fact that Cu nanowires maintain a direct electrical connection with the substrate, thereby shortening the diffusion distance for lithium insertion and facilitating electron collection and transport. It can be seen that the discharge capacities of the electrode in the 10^{th}, 20^{th} and 30^{th}cycles are 1538, 1502, 1467 mAh g^{-1} respectively. A reversible capacity as high as 1419 mAh g^{-1} after 40 cycles with the retention of about 89.1% compared with the first reversible capacity can be observed. The space among the nanowires could effectively buffer the volume change during alloying and de-alloying processes, which may be responsible for the good cycle reversibility. The rate capability performances are shown in Fig. 4c. The Cu–Ge core–shell nanowire array electrodes exhibit the discharge capacity of 1507, 1228, 1103, 1020, 979, and 842 mAh g^{-1} at 1, 2, 4, 8, 16, and 32 C (51.2 A g^{-1}), respectively (Fig. 4c). Once upon decreasing the rate from 32 C to 1 C, 98.2% of the capacity at 1 C can be recovered, indicating the superior rate cyclability of the as-prepared Cu–Ge core–shell nanowire array electrodes. The rate capability is an important parameter for many applications of batteries such as electric vehicles and portable power tools which require fast discharge and charge rates. Therefore, higher current rate cyclability of the as-prepared Cu–Ge core–shell nanowire arrays electrodes were investigated as shown in Fig. 4d. It can be seen that a capacity of 850 and 734 mAh g^{-1} can be retained after 80 cycles at a current rate of 40 C (64 A g^{-1}) and 60 C, respectively. We believe that the rate capability of our Cu–Ge core–shell nanowire array electrodes is very encouraging.[4,11,21]

The effects of the thickness of Ge films were investigated to optimize the electrochemical performance of Cu–Ge three-dimensional electrodes. Fig. 5 shows the SEM images of a series of Cu–Ge nanowire arrays with different Ge thicknesses by adjusting the depositing conditions. It can be seen from Fig. 5a and b that the surface of the Cu nanowires turns slightly rough with a sputtering time of 16 min and 32 min, respectively, indicating that a thin Ge layer may be coated. When the sputtering time was increased to 48 min, the deposited Ge layer became denser and thicker (Fig. 5c), suggesting the formation of a uniform core–shell structure. If the deposition time was further prolonged to 64 min, an excessive Ge film would cover the top of the Cu nanowire arrays as observed in Fig. 5d. Cycling performances of the Cu–Ge core–shell three dimensional electrodes with different thicknesses were tested under the same conditions (0.5 C). Fig. 6 exhibits the discharge capacity *vs.* the cycle number for the four Ge electrodes with a sputtering time ranging from 16 min to 64 min. It is indicated that there is almost no difference of behavior between the electrodes with the sputtering time from 16 min to 48 min. They all show excellent cycling stability, which could be explained by the above-mentioned advantages of the nanowire array three-dimensional electrodes. When the depositing time of Ge is increased to 64 min, excessive Ge would cover the top of the Cu nanoarrays, suggesting that there is insufficient space for buffering the volume expansion of the electrode during cycling. As a result, the capacity fading is unavailable because this sample failed to take advantage of the merits of the superior array structure efficiently.

In order to intuitively illustrate the advantages of Cu–Ge core–shell nanowire arrays as three-dimensional electrodes, the electrochemical performance of the Ge film deposited (48 min) directly on a Cu plane substrate was tested under the same conditions for comparison. It can be seen in Fig. 7a that the Ge layer on a planar Cu current collector shows rapid capacity decline and gives only a capacity of 185 mAh g^{-1} after 40 cycles. By contrast, the Cu–Ge three-dimensional electrode exhibits much larger capacity and better cycling performance than the Ge film on a planar Cu electrode, indicating the advantages of the three-dimensional electrode. Fig. 7b–d show the SEM images of the planar electrode and three-dimensional electrode after 20 cycles for comparison. It can be seen that the Ge-based active material layer is still stuck on the surface of the Cu nanowires and no appreciable change in the morphology could be noticed in the three-dimensional electrode, while strong cracks developed over the whole surface of the coating layer in the planar electrode. Therefore, the Cu–Ge three-dimensional electrode suggests the good stability, good electrical contact, and fast

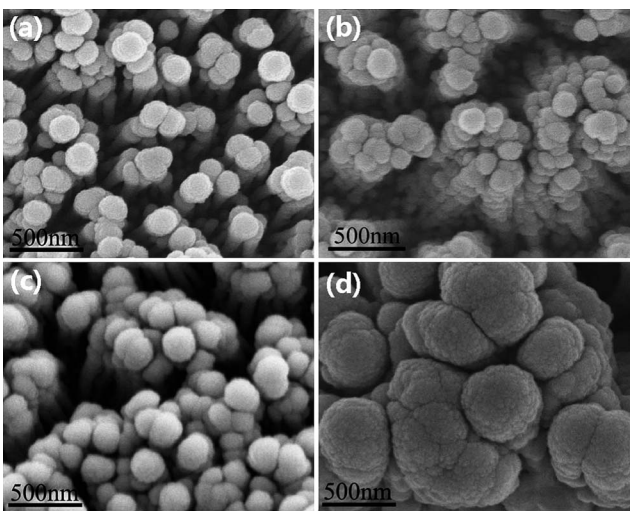

Fig. 5 SEM images of the Cu–Ge core–shell nanowire arrays with different thicknesses of Ge layer fabricated by sputtering for different times: (a) 16 min; (b) 32 min, (c) 48 min and (d) 64 min, respectively.

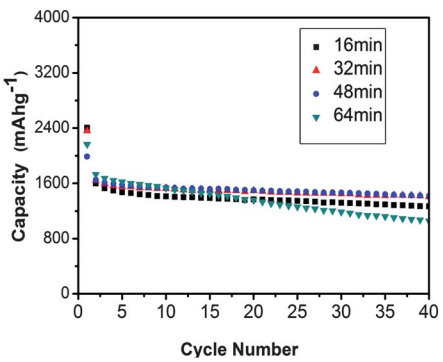

Fig. 6 Discharge capacities *versus* cycle number of the Cu–Ge three-dimensional electrode with four different thicknesses of Ge layer.

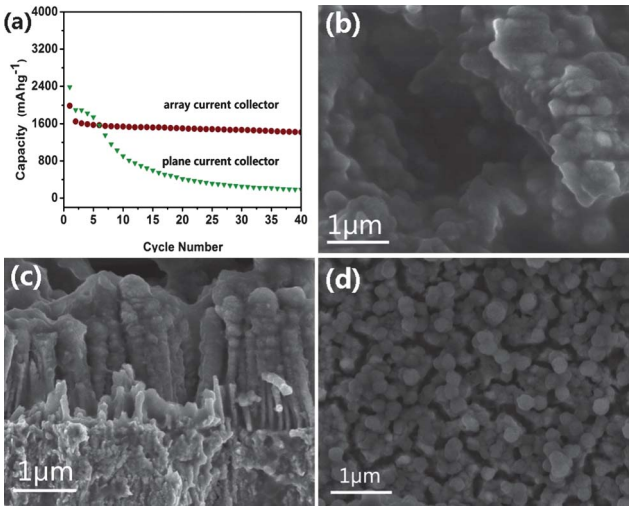

Fig. 7 (a) Cycling performance for the Cu–Ge three-dimensional electrode and Cu–Ge planar electrode at the current density of 800 mA g^{-1}; (b) SEM image of the Cu–Ge planar electrode after 20 cycles; (c), (d) top and cross-section view SEM images of the Cu–Ge three-dimensional electrode after 20 cycles.

electron transport, which may be responsible for the improved electrochemical performance.

Conclusion

In summary, Cu–Ge core–shell nanowire arrays were successfully synthesized by directly depositing a Ge layer on the surface of the pre-synthesized Cu nanowire arrays *via* an rf-sputtering method. When used as the anode materials of Li-ion batteries, the three-dimensional nanowire array electrodes delivered an initial discharge capacity of 1987 mAh g^{-1} and a Coulomb efficiency of 80.1% at a current of 0.5 C. A reversible capacity as high as 1419 mAh g^{-1} can be sustained after 40 cycles. It also exhibited an excellent rate capability with a capacity up to 850 and 734 mAh g^{-1} after 80 cycles at a current of 40 C and 60 C, respectively. The electrochemical performance of the Cu–Ge nanowire array electrode depends on the deposition parameters of the Ge layer. An excessive Ge film may induce the performance deterioration. It is believed that the excellent electrochemical performance can be attributed to the efficient buffering of the volume change, fast transport of electron and good contact to the current collector of the three-dimensional electrodes.

Acknowledgements

The authors would like to appreciate the financial support from 973 Project (No. 2007CB613403), NSFC (No. 50802086 and No. 51002133)

References

1 B. Scrosati, *Nature*, 1995, **373**, 557.
2 E. J. Hosono, T. Kudo, I. Honma, H., Matsuda and H. S. Zhou, *Nano Lett.*, 2009, **9**, 1045.
3 R. Huang, X. Fan, W. C. Zhu and J. Shen, *Appl. Phys. Lett.*, 2009, **95**, 133119.
4 C. K. Chan, X. F. Zhang and Y. Cui, *Nano Lett.*, 2008, **8**, 1.
5 J. M. Tarascon and M. Armand, *Nature*, 2001, **414**, 359.
6 Y. Wang and G. Z. Cao, *J. Mater. Chem.*, 2007, **17**, 894.
7 J. Chen, L. Xu, W. Li and X. Gou, *Adv. Mater.*, 2005, **17**, 582.
8 Q. M. Pan, H. B. Wang and Y. H. Jiang, *J. Mater. Chem.*, 2007, **17**, 329.
9 N. Du, H. Zhang, B. D. Chen, J. B. Wu, X. Y. Ma, Z. H. Liu, Y. Q. Zhang, D. R. Yang, X. H. Huang and J. P. Tu, *Adv. Mater.*, 2007, **19**, 4505.
10 Y. S. Hu, L. Kienle, Y. G. Guo and J. Maier, *Adv. Mater.*, 2006, **18**, 1421.
11 G. L. Cui, L. Gu, L. J. Zhi, N. Kaskhedikar, P. A. van Aken, K. Mullen and J. Maier, *Adv. Mater.*, 2008, **20**, 3079.
12 W. J. Weydanz, M. W. Mehrens and R. A. Huggins, *J. Power Sources*, 2003, **81**, 237.
13 L. Y. Beaulieu, T. D. Hatchard, A. Bonakdarpour, M. D. Fleischauer and J. R. Dahn, *J. Electrochem. Soc.*, 2003, **150**, A1457.
14 T. D. Hatchard and J. R. Dahn, *J. Electrochem. Soc.*, 2004, **151**, A838.
15 C. S. Fuller and J. C. Severiens, *Phys. Rev.*, 1954, **96**, 21.
16 R. A. Sharma and R. N. Seefurth, *J. Electrochem. Soc.*, 1976, **123**, 1763.
17 M. R. St. John and R. A. Huggins, *J. Electrochem. Soc.*, 1980, **127**, C136.
18 C. J. Wen, A. J. Furgala and A. F. Sammells, *J. Solid State Chem.*, 1981, **37**, 271.
19 S. Yoon, C. M. Park and H. J. Sohn, *Electrochem. Solid-State Lett.*, 2008, **11**, A42.
20 Y. S. Hu, R. D. Cakan, M. M. Titrici, J.-O. Mueller, R. Schloegl, M. Antonietti and J. Maier, *Angew. Chem., Int. Ed.*, 2008, **47**, 1645.
21 B. Gao, S. Sinha, L. Fleming and O. Zhou, *Adv. Mater.*, 2001, **13**, 816.
22 C. M. Hwang and J. W. Park, *Thin Solid Films*, 2010, **518**, 6590.
23 B. Laforge, L. L. Jodin, R. Salota and A. Billard, *J. Electrochem. Soc.*, 2008, **155**, A181.
24 P. L. Taberna, S. Mitra, P. Poizot, P. Simon and J. M. Tarascon, *Nat. Mater.*, 2006, **5**, 567.
25 A. Finke, P. Poizot, C. Guery, L. Dupont, P. L. Taberna, P. Simon and J. M. Tarascon, *Electrochem. Solid-State Lett.*, 2008, **11**, E5.
26 L. Bazina, S. Mitra, P. L. Taberna, P. Poizot, M. Gressier, M. J. Menua, A. Barnaé, P. Simona and J.-M. Tarasconb, *J. Power Sources*, 2009, **188**, 578.
27 J. Hassoun, S. Panero, P. Simon, P. L. Taberna and B. Scrosati, *Adv. Mater.*, 2007, **19**, 1632.